RETHINKING PERTURBATION PREDICTION BASELINES

Anonymous authors
Paper under double-blind review

ABSTRACT

Predicting cellular responses to genetic perturbations is central to understanding biology and unlocking more efficient drug and genetic therapy discovery. Recent approaches leverage large language models and deep learning for this task, yet simple baselines for predicting categorical outcomes—such as whether a gene is differentially expressed or up- or down-regulated—remain underexplored. We evaluate two simple baselines on Perturb-seq screens from four cell lines: a gene-based majority vote and an embedding-based k-nearest neighbors classifier. On curated benchmarks, majority vote alone achieves accuracies of 0.62–0.80, but collapses on full, unfiltered data, exposing how dataset curation can inflate model performance. On the same unfiltered data, a nearest-neighbor classifier matches LLM-based methods and remains competitive with state-of-the-art deep generative models in cross-cell-line transfer tasks. These results highlight the need for stronger baselines and for directly modeling categorical perturbation outcomes.

1 INTRODUCTION

Predicting how cells respond to drug and genetic perturbations is a key step toward building "virtual cells" that could accelerate drug discovery and precision medicine (Rood et al., 2024; Bunne et al., 2024). This goal is supported by recent technologies such as Perturb-seq (Dixit et al., 2016), which combines CRISPR-based perturbations with single-cell RNA-seq to provide interventional data on the effects of gene knockdowns on gene expression (e.g., whether a gene is differentially expressed (DE), and if so, whether it is up- or down-regulated). For instance, perturbing *ANK2*, a gene linked to neurodevelopment, led to significantly increased expression of an interneuron-specific gene module, suggesting a potential role in interneuron maturation beyond its known functions (Jin et al., 2020).

With the rise of generative AI, recent work has turned to building genomic models using pretraining strategies from large language models (Cui et al., 2023; Roohani et al., 2023), as well as directly querying LLMs such as GPT-4o/o1 and LLaMA (Wu et al., 2025; Phillips et al., 2025; Swanson et al., 2025). Alongside these modeling efforts, the importance of *careful evaluation* has become apparent. One line of work has proposed *simple yet effective baselines*, such as regularized regression, to predict the *average effect* of perturbations, showing that deep learning models often fail to outperform linear baselines on standard metrics like mean squared error (MSE) and correlation (Ahlmann-Eltze et al., 2025). Others have scrutinized evaluation practices more directly, calling for better train/test splits and distributional metrics beyond mean accuracy (Viñas Torné et al., 2025). However, most of this work has focused on predicting **continuous gene expression values**, typically after preprocessing steps such as normalization and $\log(1+x)$ transformation. Comparatively little attention has been given to **predicting categorical outcomes—whether a gene is differentially expressed, up-regulated, or down-regulated**—which are often easier to interpret biologically.

In this work, we seek to probe beyond continuous prediction metrics, as absolute transcript abundance is driven by technical rather than biological artifacts—such as platform, protocol, and normalization. In particular, we ask: (1) How well do current models perform when we convert predicted continuous gene expression values into qualitative differential expression categories? and (2) How well do models perform when we directly predict categorical DE outcomes?

Closest to our work are PerturbQA (Wu et al., 2025) and SynthPert (Phillips et al., 2025), both of which leverage LLMs to integrate prior information through retrieval-augmented generation and reasoning traces, respectively. We explore a simpler approach: direct prediction using embedding vectors in k-nearest neighbor or regularized logistic regression models. **On benchmark datasets, these methods outperform many LLM-based approaches and continuous prediction models.**

Based on our findings, we call for greater attention to downstream objectives of virtual cell models. If the goal is to predict differential expression status or changes in cell states, it may be more interpretable to model these categorical outcomes directly. Building more expressive models on our simple baselines may also yield more performant methods.

2 Methods

Following Phillips et al. (2025), we formulate perturbation outcome prediction as a three-class classification problem. Given a perturbation–gene pair (P, G), the task is to predict whether gene G under perturbation P is: (1) non-differentially expressed (`Non-DE`), (2) up-regulated (`Up`), or (3) down-regulated (`Down`). An alternative approach is to treat these as two sequential binary classification problems (Wu et al., 2025), and we found qualitatively similar conclusions.

2.1 Dataset, Processing, and Sampling

We benchmark on essential gene screens from K562, RPE1, Jurkat, and HepG2 cell lines, chosen for their widespread use in perturbation effect prediction (Nadig et al., 2025; Replogle et al., 2022), which facilitates direct comparison across methods. For each dataset, we followed prior work (Roohani et al., 2023; Adduri et al., 2025) and normalized raw UMI counts by dividing by the total counts per cell, scaling to 10,000, and applying a $\log(1 + x)$ transformation. To obtain DE statistics, we performed a Wilcoxon rank-sum test with Benjamini–Hochberg correction per perturbation, controlling the false discovery rate at $p < 0.01$. For DE pairs, the sign of the $\log$-fold change determines up- or down-regulation (see Table 1).

We consider two evaluation settings based on how non-DE pairs are handled. First, under **PerturbQA downsampling**, we follow Wu et al. (2025) and downsample non-DE pairs to address the severe class imbalance present across all four datasets (95–98% non-DE), which can bias both training and evaluation. Second, we evaluate on the **full dataset without downsampling**, reflecting the more realistic setting where no prior knowledge of class distribution is available. We annotate our results to distinguish between these two settings. In both cases, we use a 75/25 train/test split such that all test perturbations are unseen during training.

2.2 Within Cell Line Modeling

Perturbation Majority Vote. We first consider a simple majority vote rule based on the hypothesis that a gene's response to perturbation largely reflects its intrinsic properties rather than the specific perturbation applied. That is, if gene G tends to be up-regulated across most training perturbations, we predict it will also be up-regulated under a new, unseen perturbation. Formally, for each gene g, we assign the most frequent response class observed across all training perturbations:

$$\hat{y}_g = \mathrm{mode}\left(\{y_{g,p}\}_{p \in \mathcal{P}_{\mathrm{train}}}\right), \quad y_{g,p} \in \{\mathrm{Up}, \mathrm{Down}, \text{Non-DE}\}, \tag{1}$$

where $\mathcal{P}_{\mathrm{train}}$ denotes the set of training perturbations and $y_{g,p}$ is the observed DE status of gene g under perturbation p. Notably, because this baseline ignores perturbation identity entirely, it produces the same prediction for gene g regardless of which perturbation is applied. Models that fail to outperform this baseline may not be capturing meaningful perturbation-specific signal.

Weighted k-Nearest Neighbors. To incorporate perturbation-specific information, we use a weighted k-nearest neighbors (kNN) classifier with GenePT embeddings (Chen & Zou, 2023) to represent perturbations. For each query pair (P, G), we identify the k most similar training perturbations via Euclidean distance in embedding space (or equivalently the cosine similarity, since the embeddings are ℓ_2-normalized) and predict G's response through distance-weighted voting, where k is selected by 5-fold cross-validation. This baseline evaluates whether local neighborhoods in perturbation embedding space capture sufficient information for predicting gene responses.

Table 1: Perturbation dataset statistics.

	K562	**RPE1**	**HepG2**	**Jurkat**
Total pairs (M)	17.6	20.9	23.0	21.3
Non-DE (%)	96.6	95.9	97.6	98.4
Up-reg. (%)	1.44	1.51	0.99	0.50
Down-reg. (%)	1.95	2.53	1.40	1.15
Train pairs (M)	13.2	15.7	17.3	15.9
Test pairs (M)	4.4	5.2	5.8	5.3
Genes	8,561	8,748	9,623	8,881

2.3 CROSS-CELL-LINE MODELING

We evaluate cross-context generalization using three out of the four datasets: RPE1, Jurkat, and HepG2. To test the transferability of majority vote on PerturbQA-curated datasets and weighted kNN on the full datasets, we trained these predictors on one cell line and tested on another. For each target cell line, we also train STATE (Adduri et al., 2025), a representative generative AI baseline. We train on a pooled dataset of all cell lines while holding out the target's test perturbations in PerturbQA's split. We then generate single-cell predictions for held-out perturbations and call DE using the same procedure (Wilcoxon + BH at FDR < 0.01) on predicted vs. control cells. We report accuracy on both the full perturbation–gene pairs and the PerturbQA downsampled subset.

3 RESULTS

A simple majority vote achieves high predictive performance on PerturbQA datasets. The PerturbQA benchmark comprises perturbation-gene pairs filtered for high statistical significance against negative controls (Wu et al., 2025). Despite this curated dataset's widespread use for model development, we find that a simple gene-based majority vote baseline already achieves strong performance. Per-class accuracy remains consistently high across all three classes (Figure 1a), suggesting that gene-intrinsic response tendency alone is a strong indicator of expression changes in these curated datasets. The performance we gain over SUMMER (LLM accompanying the PerturbQA data) is largely from higher recall in the `Up` and `Down` classes (see Figure 4 in the Appendix).

Applying the identical predictor to the full unfiltered dataset yields drastically different results. Majority vote degenerates to predicting only the dominant non-DE class, achieving near-zero accuracy on up- and down-regulated genes (Figure 1(a); Table 2). This divergence suggests that current perturbation modeling efforts operate on datasets with considerable label noise, complicating the interpretation of reported performance gains and highlighting the need to distinguish between advances in modeling versus the benefits of data curation.

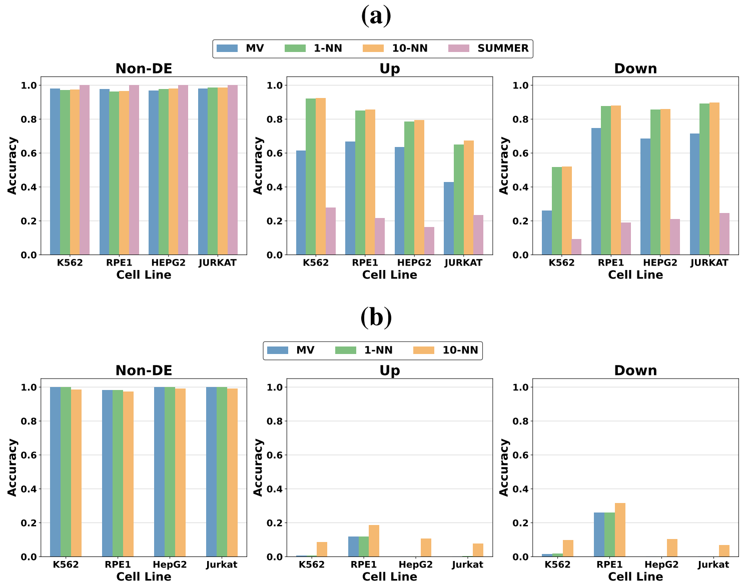

Figure 1: Per-class accuracy on (a) PerturbQA-downsampled and (b) full datasets.

Weighted K-nearest neighbors as a simple yet effective model for noisy data. Given that most perturbation models train on complete datasets, we evaluate whether incorporating perturbation-specific information can recover meaningful performance on unfiltered data. We fit a weighted K-nearest neighbors classifier using GenePT embeddings to represent perturbations—a method requiring no fine-tuning, no large-scale pretraining, and minimal computational resources. Despite operating on the challenging full dataset, 10-NN achieved balanced accuracy of 0.39–0.49 and substantially improved minority class detection: up-regulated F1 increased from near-zero to 0.11–0.27, and down-regulated F1 to 0.09–0.39 (Figure 1(b); Table 2).

To contextualize this performance, we compared against SynthPert (Phillips et al., 2025), which involves fine-tuning LLMs on self-generated chain-of-thought reasoning. On PerturbQA-sampled data, SynthPert reported an average up-regulated F1 of 0.22, comparable to our KNN model despite orders of magnitude greater complexity. Our simple distance-weighted voting scheme with a single tuning parameter k, captures much of the signal from perturbation similarity and underscores the importance of establishing strong baselines before pursuing expensive approaches.

3.1 CROSS-CELL LINE TRANSFERABILITY

To evaluate the transferability of predictors under different cellular contexts, we performed cross-cell line experiments where the models were trained on three datasets and tested on the fourth. When restricted to PerturbQA-sampled datasets (Figure 2(a)), simple neighbor-based predictors transfer robustly across-cell lines, with up-regulation accuracy ranging from 34–43% and down-regulation from 35–55%. Notably, STATE (trained on all data) underperforms the simple baselines when restricted to the subsampled data, with up-regulation accuracy below 5% across all tested cell lines.

When evaluated on the full datasets without downsampling (Figure 2(b), the class imbalance becomes severe (>95% non-DE), causing the MV baseline to predict non-DE for all pairs. In this challenging setting, both 10-NN and STATE struggle with minority class prediction, with per-class accuracy below 6% for up-regulation and below 17% for down-regulation. STATE achieves marginally higher down-regulation accuracy on RPE1 (17.3% vs 5.0%) and HepG2 (11.5% vs 6.0%), but collapses entirely on Jurkat (up-regulation: 0.1%, down-regulation: 1.8%), where the 10-NN GenePT baseline maintains more stable predictions.

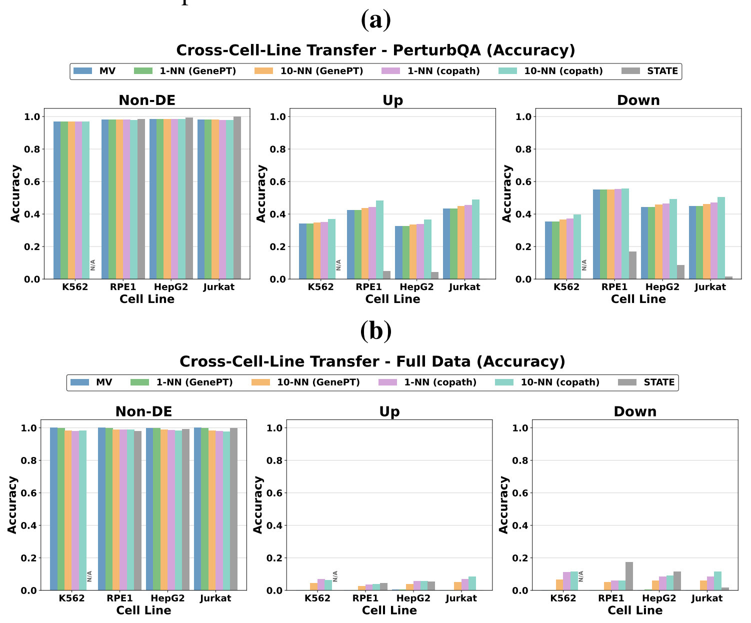

Figure 2: cross-cell-line transfer per-class accuracy on (a) PerturbQA subset and (b) full data.

4 Discussion and Conclusion

Our results show that simple baselines such as embedding-based kNN perform competitively on perturbation outcome prediction. Moreover, the strong performance of majority vote on curated data, paired with its collapse on full data, highlights the importance of careful evaluation. Our baselines do not differentiate confidence levels in the Non-DE/Up/Down labels across training perturbations, particularly for perturbations with few cells. Extending our methods to incorporate uncertainty, handle multi-gene perturbations, and testing on systematic functional-group-based splits would further strengthen our findings. Calibrating continuous models like STATE to produce categorical outputs could also offer the best of both worlds.

We advocate for routine inclusion of simple baselines with per-class metrics on Perturb-seq prediction tasks. If the downstream goal is categorical—DE status or cell state changes—modeling these outcomes directly may be more productive than discretizing continuous predictions post hoc.

REFERENCES

Abhinav K Adduri, Dhruv Gautam, Beatrice Bevilacqua, Alishba Imran, Rohan Shah, Mohsen Naghipourfar, Noam Teyssier, Rajesh Ilango, Sanjay Nagaraj, Mingze Dong, et al. Predicting cellular responses to perturbation across diverse contexts with state. *BioRxiv*, pp. 2025–06, 2025.

Constantin Ahlmann-Eltze, Wolfgang Huber, and Simon Anders. Deep-learning-based gene perturbation effect prediction does not yet outperform simple linear baselines. *Nature Methods*, 22(8): 1657–1661, Aug 2025. doi: 10.1038/s41592-025-02772-6.

Charlotte Bunne, Yusuf Roohani, Yanay Rosen, Ankit Gupta, Xikun Zhang, Marcel Roed, Theo Alexandrov, Mohammed AlQuraishi, Patricia Brennan, Daniel B Burkhardt, et al. How to build the virtual cell with artificial intelligence: Priorities and opportunities. *Cell*, 187(25):7045–7063, 2024.

Yiqun Chen and James Zou. Genept: A simple but effective foundation model for genes and cells built from chatgpt. *bioRxiv*, Oct 2023. doi: 10.1101/2023.10.16.562533.

Haotian Cui, Chloe Wang, Hassaan Maan, Kuan Pang, Fengning Luo, and Bo Wang. scgpt: Towards building a foundation model for single-cell multi-omics using generative ai. *bioRxiv*, 2023.

Atray Dixit, Oren Parnas, Biyu Li, Jenny Chen, Charles P Fulco, Livnat Jerby-Arnon, Nemanja D Marjanovic, Danielle Dionne, Tyler Burks, Raktima Raychowdhury, et al. Perturb-seq: dissecting molecular circuits with scalable single-cell rna profiling of pooled genetic screens. *cell*, 167(7): 1853–1866, 2016.

Xin Jin, Sean K Simmons, Amy Guo, Ashwin S Shetty, Michelle Ko, Lan Nguyen, Vahbiz Jokhi, Elise Robinson, Paul Oyler, Nathan Curry, et al. In vivo perturb-seq reveals neuronal and glial abnormalities associated with autism risk genes. *Science*, 370(6520):eaaz6063, 2020.

Ajay Nadig, Joseph M. Replogle, Angela N. Pogson, Mukundh Murthy, Steven A. McCarroll, Jonathan S. Weissman, Elise B. Robinson, and Luke J. O'Connor. Transcriptome-wide analysis of differential expression in perturbation atlases. *Nature Genetics*, 57(5):1228–1237, 2025. doi: 10.1038/s41588-025-02169-3. URL `https://doi.org/10.1038/s41588-025-02169-3`.

Lawrence Phillips, Marc Boubnovski Martell, Aditya Misra, Josefa Lia Stoisser, Cesar A. Prada-Medina, Rory Donovan-Maiye, and Kaspar Märtens. Synthpert: Enhancing llm biological reasoning via synthetic reasoning traces for cellular perturbation prediction, 2025. URL `https://arxiv.org/abs/2509.25346`.

Joseph M. Replogle, Reuben A. Saunders, Angela N. Pogson, Jeffrey A. Hussmann, Alexander Lenail, Alina Guna, Lauren Mascibroda, Eric J. Wagner, Karen Adelman, Gila Lithwick-Yanai, Nika Iremadze, Florian Oberstrass, Doron Lipson, Jessica L. Bonnar, Marco Jost, Thomas M. Norman, and Jonathan S. Weissman. Mapping information-rich genotype-phenotype landscapes with genome-scale perturb-seq. *Cell*, 185(14):2559–2575.e28, 2022. ISSN 0092-8674. doi: https://doi.org/10.1016/j.cell.2022.05.013. URL `https://www.sciencedirect.com/science/article/pii/S0092867422005979`.

Jennifer E Rood, Anna Hupalowska, and Aviv Regev. Toward a foundation model of causal cell and tissue biology with a perturbation cell and tissue atlas. *Cell*, 187(17):4520–4545, 2024.

Yusuf Roohani, Kexin Huang, and Jure Leskovec. Predicting transcriptional outcomes of novel multigene perturbations with gears. *Nature Biotechnology*, 2023.

Kyle Swanson, Yiqun T Chen, Aaron Jaech, and James Zou. Rl-finetuning of openai o1-mini to enhance biomedical reasoning. *bioRxiv*, pp. 2025–05, 2025.

Ramon Viñas Torné, Maciej Wiatrak, Zoe Piran, Shuyang Fan, Liangze Jiang, Sarah A Teichmann, Mor Nitzan, and Maria Brbić. Systema: a framework for evaluating genetic perturbation response prediction beyond systematic variation. *Nature Biotechnology*, pp. 1–10, 2025.

Menghua Wu, Russell Littman, Jacob Levine, Lin Qiu, Tommaso Biancalani, David Richmond, and Jan-Christian Huetter. Contextualizing biological perturbation experiments through language. In *The Thirteenth International Conference on Learning Representations*, 2025.

A Appendix

A.1 Additional results

Table 2: Per-class performance metrics for gene-based majority vote and weighted KNN (k=1, k=10) on full datasets, displayed in Figure 1(b).

		Non-DE			**Up-regulated**			**Down-regulated**		
Target	**Method**	Prec.	Recall	F1	Prec.	Recall	F1	Prec.	Recall	F1
K562	MV	0.909	0.999	0.952	0.463	0.007	0.014	0.506	0.017	0.034
	1-NN	0.909	0.999	0.952	0.450	0.007	0.015	0.507	0.019	0.036
	10-NN	0.915	0.985	0.949	0.327	0.086	0.137	0.432	0.098	0.160
RPE1	MV	0.918	0.983	0.950	0.533	0.119	0.195	0.566	0.261	0.357
	1-NN	0.918	0.984	0.950	0.534	0.119	0.195	0.568	0.261	0.358
	10-NN	0.923	0.973	0.947	0.469	0.186	0.266	0.523	0.316	0.394
HepG2	MV	0.960	1.000	0.980	0.000	0.000	0.000	0.000	0.000	0.000
	1-NN	0.960	1.000	0.980	0.094	0.000	0.000	0.031	0.000	0.000
	10-NN	0.964	0.992	0.978	0.367	0.106	0.165	0.329	0.103	0.157
Jurkat	MV	0.974	1.000	0.987	0.000	0.000	0.000	0.000	0.000	0.000
	1-NN	0.974	1.000	0.987	0.448	0.003	0.005	0.077	0.001	0.003
	10-NN	0.976	0.991	0.983	0.193	0.078	0.111	0.155	0.068	0.094

Table 3: cross-cell line transfer performance. Cross-domain values are averaged across all source cell lines. “All genes” evaluates on the full target gene set (unseen genes default to Non-DE for gene-based majority vote); “Overlap genes” restricts to genes present in the source training data.

	Accuracy		**Balanced Accuracy**		**Macro F1**	
Target	**All**	**Overlap**	**All**	**Overlap**	**All**	**Overlap**
Gene-based majority vote (PerturbQA)						
K562	0.875	0.880	0.480	0.547	0.490	0.541
RPE1	0.893	0.894	0.553	0.646	0.596	0.665
HepG2	0.883	0.889	0.485	0.606	0.528	0.627
Jurkat	0.888	0.879	0.534	0.631	0.571	0.641
Embedding-based KNN (K=1, full dataset)						
K562	0.948	0.943	0.445	0.453	0.455	0.460
RPE1	0.947	0.943	0.412	0.422	0.427	0.434
HepG2	0.957	0.953	0.450	0.460	0.427	0.430
Jurkat	0.957	0.952	0.474	0.482	0.422	0.423

Table 4: cross-cell-line transfer per-class performance on full data.

		Non-DE			Up-regulated			Down-regulated		
Target	**Method**	Prec.	Recall	F1	Prec.	Recall	F1	Prec.	Recall	F1
K562	MV	0.919	1.000	0.958	0.000	0.000	0.000	0.000	0.000	0.000
	1-NN (GenePT)	0.919	1.000	0.957	0.111	0.000	0.001	0.170	0.001	0.002
	10-NN (GenePT)	0.922	0.984	0.952	0.172	0.045	0.071	0.293	0.067	0.110
	STATE					*N/A*				
RPE1	MV	0.907	1.000	0.951	0.000	0.000	0.000	0.000	0.000	0.000
	1-NN (GenePT)	0.907	1.000	0.951	0.550	0.001	0.001	0.232	0.002	0.003
	10-NN (GenePT)	0.910	0.990	0.948	0.206	0.027	0.048	0.320	0.050	0.087
	STATE	0.945	0.979	0.962	0.182	0.046	0.074	0.305	0.173	0.221
HepG2	MV	0.959	1.000	0.979	0.102	0.003	0.006	0.000	0.000	0.000
	1-NN (GenePT)	0.960	0.999	0.979	0.103	0.004	0.009	0.165	0.003	0.006
	10-NN (GenePT)	0.961	0.990	0.975	0.118	0.039	0.058	0.211	0.060	0.094
	STATE	0.969	0.992	0.980	0.381	0.054	0.095	0.265	0.115	0.160
Jurkat	MV	0.974	1.000	0.987	0.000	0.000	0.000	0.000	0.000	0.000
	1-NN (GenePT)	0.974	0.999	0.987	0.026	0.001	0.002	0.099	0.002	0.004
	10-NN (GenePT)	0.976	0.984	0.980	0.062	0.050	0.055	0.101	0.059	0.075
	STATE	0.974	0.999	0.986	0.016	0.001	0.001	0.232	0.018	0.033

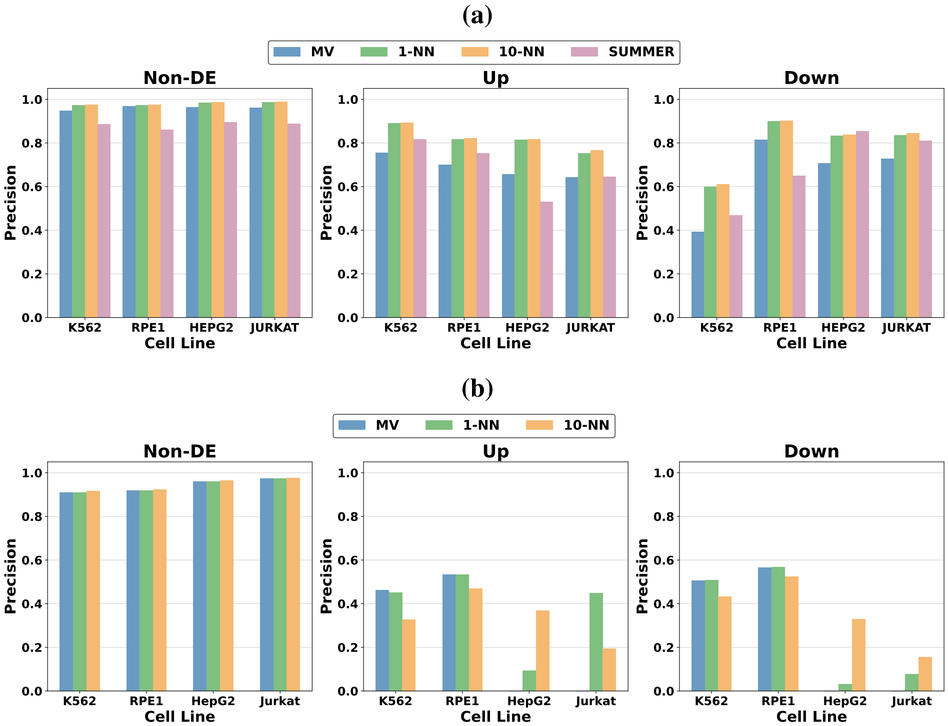
(a)

(b)

Figure 3: Per-class precision on (a) PerturbQA-downsampled and (b) full datasets.

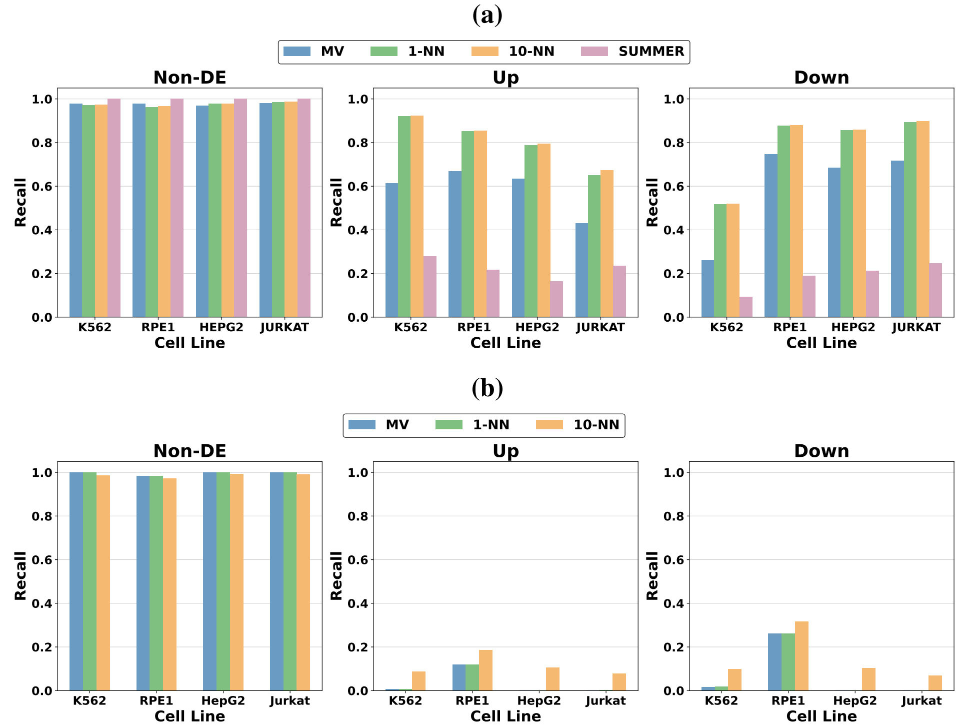

Figure 4: Per-class recall on (a) PerturbQA-downsampled and (b) full datasets.